© 1997 The Chemical Society of Japan Bull. Chem. Soc. Jpn., 70, 987—991 (1997) 987

# Density and Volumetric Behavior of 1,2-Dimethoxyethane + Water Binary Mixtures from −10 to 80 °C

**Andrea Marchetti, Lorenzo Tassi,* and Alessandro Ulrici**

Department of Chemistry, University of Modena, via G. Campi, 183-41100 Modena, Italy

(Received July 8, 1996)

The densities ($\rho$) and excess molar volumes ($V^E$) for 1,2-dimethoxyethane + water binary mixtures were determined, when possible, at 19 different temperatures ranging from −10 up to +80°C. The experimental measurements were used to test some empirical relations giving the dependence of the density on the temperature and binary composition: $\rho=\rho(t)$, $\rho=\rho(X_1)$, and $\rho=\rho(t,X_1)$. Furthermore, the results of $V^E$ calculations are discussed in terms of the influence of interactions between the components, of the order and degree of packing in the mixtures, and of the free-volume differences.

In recent years, specific intermolecular interactions in binary liquid mixtures, both the non-hydrogen and hydrogen bonding types, were investigated in our laboratories based on the thermophysical measurable properties, such as the density ($\rho$), viscosity (either kinematic, $\nu$/cSt (1 St $= 10^{-4}$ m$^2$s$^{-1}$), or dynamic, $\eta$/cP (1 cP=mPa S)), dielectric constant ($\varepsilon$), refractive index ($n$), and some related quantities. In order to achieve such an extensive variety of results we chose for this research program some nonaqueous solvents, which were mixed with one another and with water.[1—5]

Particular attention was paid in our previous studies to some 1,2-ethanediyl-derivatives, such as 1,2-ethanediol (ED), 2-methoxyethanol (ME), and 1,2-dimethoxyethane (DME), among other species. Along these research lines, we present here a detailed inspection of the densities and related volumic properties of DME (component 1) + water (W, component 2) binary mixtures.

DME is one of the simplest amphiphilic species, which is only slightly polar ($\mu = 1.17$ D (1 D $= 3.335\times10^{-30}$ C m))[6] and quite miscible with water, even if very consistent hydrophobic hydration effects are present.[7] The composition dependence of the thermophysical properties of the mixed-nonelectrolytic systems, along with the spectroscopic techniques, has proven to be very informative in helping us to understand the nature and extent of the molecular aggregation and resulting patterns from the intermolecular interactions between the components.[8,9] Even though DME is a very important nonaqueous species for a variety of technical applications[10] and electrochemical studies,[11] it seems to us that the thermophysical properties of the DME/W binary system have only been slightly reviewed;[12,13] this fact encouraged us to perform some extensive investigations over a fairly large temperature range ($-10\leq t/°\mathrm{C}\leq80$).

## Experimental

**Materials.** 1,2-Dimethoxyethane, containing less than 0.10% by weight of water, determined by Karl–Fischer titrations, was a Carlo Erba (Milan) high-purity grade reagent. This solvent was further purified by double-fractional distillation over $LiAlH_4$ to eliminate any traces of acids and peroxides, and to reduce the water content; only the middle fraction (bp 83 °C) was kept for the measurements. The purified solvent was preserved over 3 Å molecular sieves for many days before use. The final purity was checked by gas chromatography (99.7%), which confirmed the absence of other significant organic components. The water used to prepare the mixtures was deionized by a MilliQ-plus apparatus (Millipore), and had a specific conductance $\leq 0.70/\mu\mathrm{S\,cm^{-1}}$ at 25 °C.

**Apparatus and Procedures.** The mixtures were prepared by weight on a Mettler PM 4800 Δ-range balance just before use, operating in a dry box to avoid atmospheric moisture. The probable estimated error in the DME mole fraction ($X_1$) was less than $1.5\times10^{-4}$. The densities were measured with a digital densimeter (Anton Paar, Model DMA 60) equipped with a density measuring cell (DMA 602) with a sensitivity of $1\times10^{-6}/\mathrm{g\,cm^{-3}}$.

The measuring cell was standardized with calibrating fluids of known density: dried air, redistilled water, and mercury.[14,15]

The overall experimental standard deviation ($\sigma(\rho)$) was approximately equal to $\pm1.5\times10^{-6}/\mathrm{g\,cm^{-3}}$, while the estimated accuracy (95% confidence interval) was $\pm3\times10^{-6}/\mathrm{g\,cm^{-3}}$.

The DMA 602 density measuring system was embodied in a perspex box air-thermostated at the same working temperature as the measuring cell. The temperature of the measurement equipment was maintained constant within ±0.02 °C by means of two Lauda K2R thermostatic baths in cascade. The thermal control was checked by a thermoresistance Pt 100 (Tersid, Milan) inserted into the jacket of the measuring cell, located near to the sample tube, and the resistance values were measured by a Wayne Kerr 6425 Precision Component Analyzer.

## Results and Discussion

For comparison purposes, Table 1 summarizes some $\rho$ values taken from the literature for the DME pure species. As can be seen, there is a fairly good agreement between the present and previously reported data, the only exception being the reference value provided by Gmehling et al.[16]

Table 2 presents the experimental data of the densities

Table 1. Reference Density Values ($\rho$/g cm$^{-3}$) for DME at 25 °C

| $\rho$/g cm$^{-3}$ | Technique | Ref. |
|---|---|---|
| 0.86370 | Oscillating tube | 16 |
| 0.8612 | Oscillating tube | 23 |
| 0.8613 | Pycnometer | 24 |
| 0.861506 | Oscillating tube | This work |

($\rho$/g cm$^{-3}$) for the two pure solvents and 9 binary mixtures of theirs at 19 temperatures over the range −10 up to 80 °C, with a thermal scanning of 5 °C. For the sake of brevity, the letters A,B,···M which appear along with the text represent the 11 investigated liquid mixtures. Table 2 lacks some $\rho$ values at lower temperatures and in the water-rich region, because phase separation occurs.

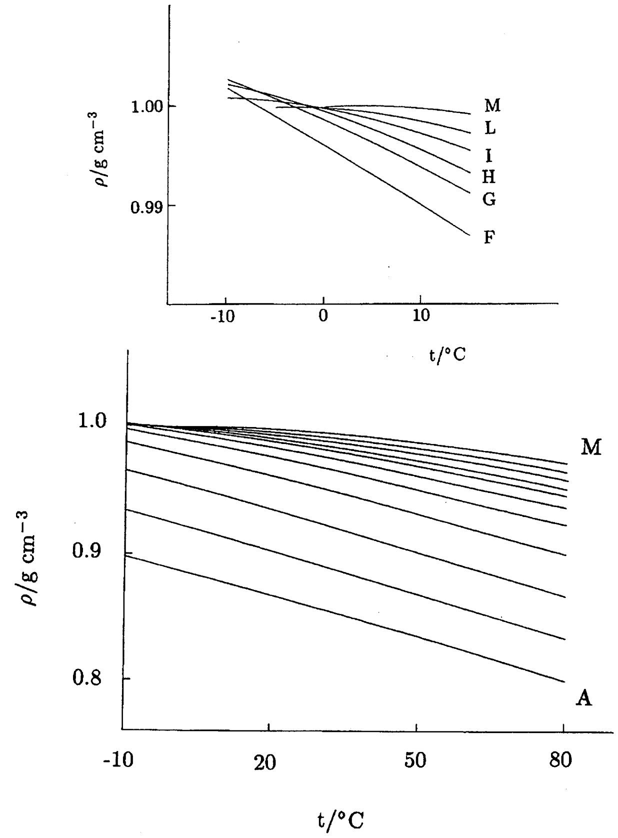

Fig. 1. Plots of density ($\rho$/g cm$^{-3}$) against $t$/°C for the DME (1)/W (2) binary mixtures.

A look at the trend of $\rho=\rho(t)$ should help the readers to understand the quite singular behavior of this solvent system (Fig. 1). It is well known that curve M (pure water) shows a maximum in the low-temperature region; this fact seems to be quite unique for this liquid species. On the contrary, we have observed that all other curves, corresponding to our selected binary compositions, are monotonously decreasing functions of the temperature in the investigated range. In order to represent in analytical form these trends, the dependence of the $\rho$ data on the temperature ($t$/°C) for each liquid mixture has been studied by applying the relation.[15]

$$\rho(t)=\sum_{0}^{k} a_k t^k, \tag{1}$$

where $a_k$ are empirical coefficients determined by a multilinear regression package, TSP.[17] The $a_k$ adjustment parameters (for $0 \leq k \leq 4$) are listed in Table 3, along with the standard deviation ($\sigma(\rho)$/g cm$^{-3}$) for each mixture. The suitability of Eq. 1 for predictive calculations in the experimental data gaps

Table 2. Binary Composition and Experimental Densities ($\rho$/g cm$^{-3}$) for the DME (1)+W (2) Solvent System at Various Temperatures

| $X_1$ = | 1.0000 | 0.6024 | 0.4029 | 0.2896 | 0.2048 | 0.1458 | 0.0999 | 0.0736 | 0.0411 | 0.0187 | 0.0000 |
|---|---|---|---|---|---|---|---|---|---|---|---|
| $V_1/V_2$%$^{a)}$ = | 100/0 | 90/10 | 80/20 | 70/30 | 60/40 | 50/50 | 40/60 | 30/70 | 20/80 | 10/90 | 0/100 |
| $t$/°C | A | B | C | D | E | F | G | H | I | L | M$^{b)}$ |
| −10 | 0.897853 | 0.934394 | 0.965744 | 0.987843 | 0.998012 | 1.001776 | 1.002653 | 1.002148 | 1.000783 | — | — |
| −5 | 0.892768 | 0.929302 | 0.961103 | 0.983545 | 0.994455 | 0.998846 | 1.000651 | 1.000921 | 1.000436 | 0.999803 | — |
| 0 | 0.887723 | 0.924026 | 0.956238 | 0.979198 | 0.990914 | 0.995949 | 0.998505 | 0.999408 | 0.999712 | 0.999748 | 0.999834 |
| 5 | 0.882581 | 0.918657 | 0.951130 | 0.974883 | 0.987359 | 0.993049 | 0.996209 | 0.997582 | 0.998588 | 0.999239 | 0.999964 |
| 10 | 0.877354 | 0.913195 | 0.945866 | 0.970474 | 0.983783 | 0.990047 | 0.993796 | 0.995495 | 0.997137 | 0.998374 | 0.999700 |
| 15 | 0.872125 | 0.907627 | 0.940442 | 0.966001 | 0.980101 | 0.986914 | 0.991192 | 0.993226 | 0.995448 | 0.997186 | 0.999100 |
| 20 | 0.866875 | 0.902034 | 0.934907 | 0.961418 | 0.976283 | 0.983701 | 0.988444 | 0.990818 | 0.993573 | 0.995770 | 0.998204 |
| 25 | 0.861506 | 0.896369 | 0.929310 | 0.956757 | 0.972361 | 0.980381 | 0.985579 | 0.988247 | 0.991479 | 0.994159 | 0.997045 |
| 30 | 0.856097 | 0.890671 | 0.923671 | 0.951947 | 0.968299 | 0.976863 | 0.982562 | 0.985518 | 0.989267 | 0.992280 | 0.995647 |
| 35 | 0.850680 | 0.884938 | 0.918012 | 0.946999 | 0.964037 | 0.973227 | 0.979408 | 0.982708 | 0.986915 | 0.990301 | 0.994032 |
| 40 | 0.845124 | 0.879199 | 0.912327 | 0.941927 | 0.959678 | 0.969457 | 0.976184 | 0.979787 | 0.984432 | 0.988116 | 0.992216 |
| 45 | 0.839575 | 0.873455 | 0.906646 | 0.936729 | 0.955168 | 0.965553 | 0.972765 | 0.976704 | 0.981805 | 0.985822 | 0.990213 |
| 50 | 0.833956 | 0.867678 | 0.901014 | 0.931478 | 0.950598 | 0.961569 | 0.969276 | 0.973539 | 0.979057 | 0.983416 | 0.988036 |
| 55 | 0.828247 | 0.861897 | 0.895335 | 0.926140 | 0.945944 | 0.957428 | 0.965661 | 0.970289 | 0.976170 | 0.980809 | 0.985695 |
| 60 | 0.822468 | 0.856070 | 0.889638 | 0.920769 | 0.941216 | 0.953281 | 0.961976 | 0.966853 | 0.973059 | 0.978072 | 0.983199 |
| 65 | 0.816676 | 0.850241 | 0.883900 | 0.915414 | 0.936557 | 0.949064 | 0.958140 | 0.963281 | 0.969800 | 0.975123 | 0.980555 |
| 70 | 0.810830 | 0.844389 | 0.878135 | 0.910112 | 0.931964 | 0.944812 | 0.954170 | 0.959492 | 0.966313 | 0.971951 | 0.977770 |
| 75 | 0.804947 | 0.838470 | 0.872248 | 0.904885 | 0.927481 | 0.940649 | 0.950153 | 0.955483 | 0.962502 | 0.968536 | 0.974899 |
| 80 | 0.799064 | 0.832435 | 0.866260 | 0.899773 | 0.923257 | 0.936618 | 0.945976 | 0.951260 | 0.958407 | 0.964853 | 0.971798 |

a) At 20 °C. b) Refs. 14 and 15.

Table 3. Coefficients $a_k$ and Standard Deviations $\sigma(\rho)/\text{g cm}^{-3}$ of Eq. 1 for the DME (1)+W (2) Binary Mixtures

| Mixture | $a_0$ | $10^5\ a_1$ | $10^7\ a_2$ | $10^9\ a_3$ | $10^{11}\ a_4$ | $10^5\ \sigma(\rho)$ |
|---|---|---|---|---|---|---|
| A | 0.887691 | −102.331 | −7.69410 | −8.40221 | 5.97302 | 2.2 |
| B | 0.924039 | −106.350 | −24.4751 | 32.8031 | −18.6476 | 1.2 |
| C | 0.956250 | −100.054 | −45.9610 | 70.3651 | −40.4193 | 1.6 |
| D | 0.979209 | −86.3538 | −4.49789 | −48.8099 | 42.8065 | 1.7 |
| E | 0.990914 | −70.5480 | −2.21207 | −63.9869 | 56.0385 | 1.3 |
| F | 0.995967 | −58.2099 | −7.64174 | −46.8428 | 39.2534 | 1.9 |
| G | 0.998523 | −44.3800 | −31.6647 | 8.07095 | −2.19405 | 1.8 |
| H | 0.999388 | −33.7969 | −55.4670 | 58.4372 | −37.8971 | 1.6 |
| I | 0.999688 | −19.0366 | −71.7713 | 80.8326 | −52.5339 | 1.7 |
| L | 0.999734 | −6.00873 | −84.3309 | 87.6002 | −51.1873 | 1.6 |
| M | 0.999847 | 5.92545 | −79.9825 | 51.2804 | −19.1635 | 1.4 |

in the present case is ascertained by an average uncertainty of $\overline{\Delta\rho}=\pm 0.000013\ \text{g cm}^{-3}$, evaluated as

$$\overline{\Delta\rho} = \frac{1}{N}\sum_{N} |\rho_{\text{exptl}} - \rho_{\text{calcd}}|, \qquad (2)$$

where $N$ (206) are the values gives in Table 2.

The next step of our investigation was a study of the dependence $\rho=\rho(X_i)$; therefore the $\rho$ values are plotted against $X_2$ in Fig. 2. Literature is quite scarce on reliable models about this question. A critical review of the equations used to predict the saturated liquid density was given by Spencer and Adler.[18] Unfortunately, their extensive evaluation of generalized methods for this purpose is only appliable to pure compounds, even for in a wide range of experimental conditions. Therefore, in the absence of well-tested interpretative models for binary mixtures, the experimental values of $\rho$ for this solvent system were fitted by a least-squares method with a polynomial function in the form

$$\rho(X_1) = \sum_{0}^{j} b_j X_1^j, \qquad (3)$$

whose the $b_j$ coefficients are listed in Table 4 along with the standard deviations ($\sigma(\rho)$) at each fitting temperature. Equation 3 recalculates the initial $\rho$ data with a mean error

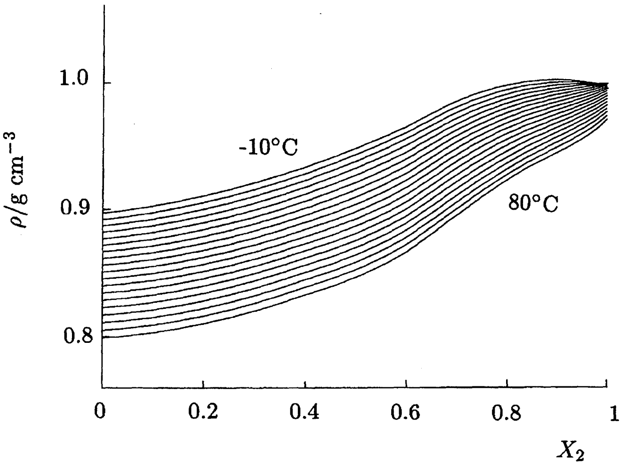

Fig. 2. Plots of density ($\rho/\text{g cm}^{-3}$) against $X_2$ for the DME (1)/W (2) binary mixtures.

Table 4. Coefficients $b_j$ and Standard Deviations $\sigma(\rho)/\text{g cm}^{-3}$ of Eq. 3 for the DME (1)+W (2) Binary Mixtures at Various Temperatures

| $t/°\text{C}$ | $b_0$ | $10^2\ b_1$ | $10^2\ b_2$ | $10\ b_3$ | $10\ b_4$ | $10\ b_5$ | $10\ b_6$ | $10^4\ \sigma(\rho)$ |
|---|---|---|---|---|---|---|---|---|
| −10 | *0.996572* | 14.2561 | −114.831 | 43.7321 | −13.9106 | 182.818 | −86.5692 | 1.0 |
| −5 | *0.998634* | 7.25420 | −71.3936 | 26.1606 | −91.0094 | 138.595 | −68.3911 | 0.9 |
| 0 | 0.999736 | 1.28311 | −30.0447 | 8.01678 | −49.0428 | 92.4949 | −49.7132 | 1.5 |
| 5 | 0.999843 | −2.27839 | −14.1509 | 2.96843 | −40.3033 | 85.3138 | −47.5089 | 1.5 |
| 10 | 0.999580 | −5.76181 | 4.43672 | −3.89130 | −27.3065 | 73.8705 | −43.7623 | 1.5 |
| 15 | 0.998980 | −9.05091 | 23.2436 | −11.2352 | −13.0028 | 61.0895 | −39.5391 | 1.6 |
| 20 | 0.998082 | −12.0835 | 40.7873 | −18.3070 | 1.08111 | 48.3016 | −35.2583 | 1.7 |
| 25 | 0.996914 | −14.8124 | 55.8132 | −24.4171 | 13.4280 | 36.9749 | −31.4398 | 1.8 |
| 30 | 0.995503 | −17.2102 | 67.5423 | −29.1511 | 23.1720 | 27.8942 | −28.3422 | 1.9 |
| 35 | 0.993874 | −19.2981 | 75.9160 | −32.4478 | 30.2169 | 21.0755 | −25.9384 | 2.1 |
| 40 | 0.992048 | −21.1086 | 81.2697 | −34.4880 | 35.0559 | 15.9026 | −23.9557 | 2.1 |
| 45 | 0.990040 | −22.7077 | 84.4461 | −35.6745 | 38.5725 | 11.4786 | −22.0552 | 2.1 |
| 50 | 0.987866 | −24.1921 | 86.8924 | −36.7613 | 42.5328 | 5.90870 | −19.4897 | 2.1 |
| 55 | 0.985535 | −25.6890 | 90.5597 | −38.7356 | 49.1410 | −3.05299 | −15.4125 | 2.0 |
| 60 | 0.983056 | −27.3397 | 97.7409 | −42.7693 | 61.0020 | −18.0351 | −8.84339 | 1.9 |
| 65 | 0.980430 | −29.3328 | 111.547 | −50.4760 | 81.7673 | −42.7918 | 1.64162 | 1.8 |
| 70 | 0.977660 | −31.8680 | 135.327 | −63.5772 | 115.257 | −81.1604 | 17.4662 | 1.8 |
| 75 | 0.974741 | −35.1876 | 173.170 | −84.1856 | 166.196 | −137.929 | 40.4218 | 1.9 |
| 80 | 0.971667 | −39.5486 | 229.482 | −114.572 | 239.618 | −218.142 | 72.3761 | 2.0 |

of $\overline{\Delta\rho}=\pm 0.000088$ g cm$^{-3}$. In this table the slanted values, relative to the lowest temperatures, were obtained by fitting incomplete data sets; therefore, the $b_0$ slanted parameters are not related to the density of pure W species.

Now, Eqs. 1 and 3 may be conveniently combined as

$$\rho(t,X_1)=\sum_{0}^{k}\sum_{0}^{j}c_{kj}t^kX_1^j, \tag{4}$$

to provide a single bivariant function which interpolates the experimental values over the entire investigated temperature and composition ranges. The recognition ability associated with this three-dimensional model is ascertained by an average uncertainty of $\overline{\Delta\rho}=\pm 0.000093$ g cm$^{-3}$. The empirical coefficients ($c_{kj}$) are listed in Table 5. It is obvious that utmost care was needed when applying all of the fitting equations, namely Eqs. 1, 3, and 4, for predictive calculations in order to avoid extrapolated values without physical meaning in temperature ($-10\leq t/°\mathrm{C}\leq 0$) and composition ($0.0411>X_1\geq 0$) domains where separation phases occurred (see Table 2).

Table 5. Coefficients $c_{kj}$ and Standard Deviations $\sigma(\rho)$/g cm$^{-3}$ of Eq. 4 for the DME (1)+W (2) Binary System[a)]

| $k_j$ | Variable | $c_{kj}$ |
|---|---|---|
| 00 | | 0.999596 |
| 01 | $X_1$ | $1.87247\times 10^{-2}$ |
| 02 | $X_1^2$ | $-3.74172\times 10^{-1}$ |
| 03 | $X_1^3$ | 1.19128 |
| 04 | $X_1^4$ | −5.87128 |
| 05 | $X_1^5$ | 10.3489 |
| 06 | $X_1^6$ | −5.42534 |
| 10 | $t$ | $9.04293\times 10^{-5}$ |
| 11 | $tX_1$ | $-8.34298\times 10^{-3}$ |
| 12 | $tX_1^2$ | $4.26631\times 10^{-2}$ |
| 13 | $tX_1^3$ | $-1.54567\times 10^{-1}$ |
| 14 | $tX_1^4$ | $3.13018\times 10^{-1}$ |
| 15 | $tX_1^5$ | $-3.09955\times 10^{-1}$ |
| 16 | $tX_1^6$ | $1.16070\times 10^{-1}$ |
| 20 | $t^2$ | $-9.68326\times 10^{-6}$ |
| 21 | $t^2X_1$ | $5.11315\times 10^{-5}$ |
| 22 | $t^2X_1^2$ | $3.12684\times 10^{-4}$ |
| 23 | $t^2X_1^3$ | $-2.41162\times 10^{-3}$ |
| 24 | $t^2X_1^4$ | $4.61307\times 10^{-3}$ |
| 25 | $t^2X_1^5$ | $-3.01726\times 10^{-3}$ |
| 26 | $t^2X_1^6$ | $4.60912\times 10^{-4}$ |
| 30 | $t^3$ | $8.20490\times 10^{-8}$ |
| 31 | $t^3X_1$ | $8.70296\times 10^{-7}$ |
| 32 | $t^3X_1^2$ | $-2.69476\times 10^{-5}$ |
| 33 | $t^3X_1^3$ | $1.41488\times 10^{-4}$ |
| 34 | $t^3X_1^4$ | $-2.86275\times 10^{-4}$ |
| 35 | $t^2X_1^5$ | $2.47727\times 10^{-4}$ |
| 36 | $t^3X_1^6$ | $-7.69533\times 10^{-5}$ |
| 40 | $t^4$ | $-3.71887\times 10^{-10}$ |
| 41 | $t^4X_1$ | $-1.26521\times 10^{-8}$ |
| 42 | $t^4X_1^2$ | $2.69405\times 10^{-7}$ |
| 43 | $t^4X_1^3$ | $-1.39649\times 10^{-6}$ |
| 44 | $t^4x_1^4$ | $2.96916\times 10^{-6}$ |
| 45 | $t^4X_1^5$ | $-2.79877\times 10^{-6}$ |
| 46 | $t^4x_1^6$ | $9.69779\times 10^{-7}$ |

a) $\sigma(\rho)=1.2\times 10^{-4}$.

**Excess Molar Volume.** The molar volume ($V$/cm$^3$ mol$^{-1}$) of the solutions and related excess property ($V^{\mathrm{E}}$/cm$^3$ mol$^{-1}$) can be evaluated by converting the density values using the equation[19)]

$$V^{\mathrm{E}}=\frac{X_1M_1+X_2M_2}{\rho}-\left(\frac{X_1M_1}{\rho_1}+\frac{X_2M_2}{\rho_2}\right), \tag{5}$$

where $M_i$ and $\rho_i$ are the molar masses ($M_1$=90.120; $M_2$=18.015) and densities of pure species at each temperature. They were smoothed by an equation of the type[20)]

$$V^{\mathrm{E}}=X_1X_2\sum_{0}^{n}d_n(X_2-X_1)^n. \tag{6}$$

The coefficients ($d_n$ ($n$=0, 1, 2, 3)) and the standard deviations ($\sigma(V^{\mathrm{E}})$/cm$^3$ mol$^{-1}$) are summarized in Table 6. This relationship recalculates the $V^{\mathrm{E}}$ quantities within $\overline{\Delta V^{\mathrm{E}}}=\pm 0.014$ cm$^3$ mol$^{-1}$ over all of the 187 initial data, and taking values in the $0.000\leq\Delta V^{\mathrm{E}}/\mathrm{cm^3\,mol^{-1}}\leq 0.047$ range. A more convenient graphical representation of the above equation is shown in Fig. 3, where, for clarity the experimental points have been omitted. As one can see, all of the curves show a pronounced minimum which seems to be slightly sensitive to temperature, and that is centered at $X_2\simeq 0.66$.

Different effects of different signs may contribute to $V^{\mathrm{E}}$. In the mixtures investigated here, we can recognize at least three different important contributions ($\pm\delta V^{\mathrm{E}}$): i) the breaking of liquid order in mixing ($-\delta V^{\mathrm{E}}$); ii) favorable ($-\delta V^{\mathrm{E}}$) and/or unfavorable ($+\delta V^{\mathrm{E}}$) interactions between the substituent and skeletal groups; iii) geometric effects, such as differences in the molecular volume and in free volume ($-\delta V^{\mathrm{E}}$) between the components in the liquid state (molar volumes are 104.608 and 18.068 cm$^3$ at 25 °C for DME and W, respectively).[21,22)]

Table 6. Coefficients $d_n$ and Standard Deviations $\sigma(V^{\mathrm{E}})$/cm$^3$ mol$^{-1}$ of Eq. 6 for the DME (1)+W (2) Binary Systems at Various Temperatures

| $t$/°C | $d_0$ | $d_1$ | $d_2$ | $d_3$ | $10^2\ \sigma(V^{\mathrm{E}})$ |
|---|---|---|---|---|---|
| 0 | −8.704 | −7.117 | −5.702 | 11.192 | 2.0 |
| 5 | −8.548 | −7.230 | −6.429 | 11.980 | 2.1 |
| 10 | −8.364 | −7.352 | −7.583 | 13.202 | 2.1 |
| 15 | −8.166 | −7.475 | −8.969 | 14.637 | 2.2 |
| 20 | −7.967 | −7.595 | −10.431 | 16.114 | 2.4 |
| 25 | −7.777 | −7.708 | −11.854 | 17.567 | 2.5 |
| 30 | −7.605 | −7.808 | −13.137 | 18.701 | 2.5 |
| 35 | −7.455 | −7.897 | −14.222 | 19.646 | 2.6 |
| 40 | −7.331 | −7.976 | −15.082 | 20.315 | 2.7 |
| 45 | −7.234 | −8.041 | −15.744 | 20.744 | 2.7 |
| 50 | −7.161 | −8.099 | −16.244 | 20.986 | 2.6 |
| 55 | −7.108 | −8.153 | −16.680 | 21.163 | 2.6 |
| 60 | −7.066 | −8.208 | −17.188 | 21.440 | 2.5 |
| 65 | −7.024 | −8.273 | −17.949 | 22.036 | 2.3 |
| 70 | −6.967 | −8.357 | −19.185 | 23.217 | 2.1 |
| 75 | −6.876 | −8.471 | −21.182 | 25.323 | 1.9 |
| 80 | −6.727 | −8.631 | −24.262 | 28.740 | 1.7 |

For comparison purposes, Fig. 4 shows the trend of $V^{\mathrm{E}}$

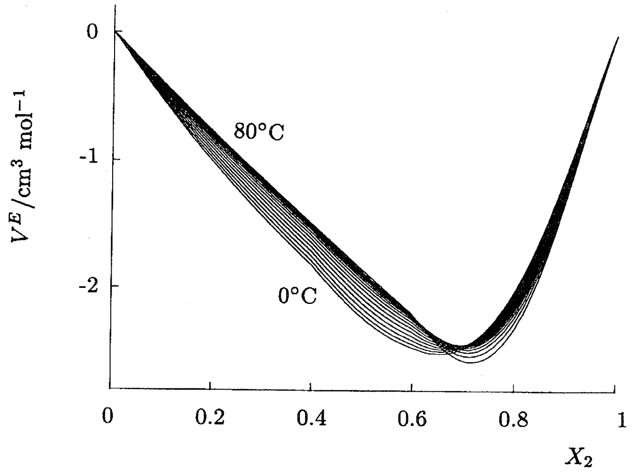

Fig. 3. Excess molar volume ($V^E$/cm$^3$ mol$^{-1}$) against W mole fraction ($X_2$) for the DME(1)/W(2) binary mixtures at various temperatures ranging from 0 to 80 °C.

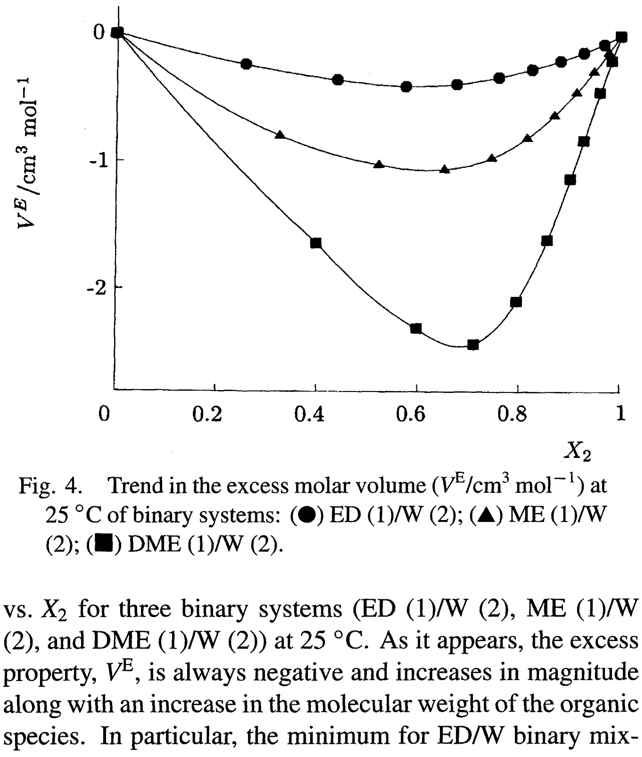

Fig. 4. Trend in the excess molar volume ($V^E$/cm$^3$ mol$^{-1}$) at 25 °C of binary systems: (●) ED (1)/W (2); (▲) ME (1)/W (2); (■) DME (1)/W (2).

vs. $X_2$ for three binary systems (ED (1)/W (2), ME (1)/W (2), and DME (1)/W (2)) at 25 °C. As it appears, the excess property, $V^E$, is always negative and increases in magnitude along with an increase in the molecular weight of the organic species. In particular, the minimum for ED/W binary mixtures is centered at $X_2 \simeq 0.6$, and its intensity is about $-0.5$ cm$^3$ mol$^{-1}$. On the other hand, ME/W and DME/W show a minimum centered at $X_2 \simeq 0.66$, whose intensities are about $-1$ and $-2.5$ cm$^3$ mol$^{-1}$, respectively.

As a concluding remark, we can recognize that changes in the excess mixing properties, such as the dielectric constant ($\varepsilon^E$)[2] and molar volume ($V^E$), confirm the presence, in these nonelectrolytic solutions, of a stable complex adduct of the type 1DME·2W, that is thermostable at all of the temperatures investigated over the range $0 \leq t/°C \leq 80$.

The authors would like to thank Prof. Carlo Preti for his generous support, guidance and approval on this research program. The Ministero dell'Università e della Ricerca Scientifica e Tecnologica (M.U.R.S.T.) and the CNR of Italy are gratefully acknowledged for the financial support.

## References

1) G. C. Franchini, A. Marchetti, M. Tagliazucchi, L. Tassi, and G. Tosi, *J. Chem. Soc., Faraday Trans. 1*, **87**, 2583 (1991).

2) L. Marcheselli, A. Marchetti, M. Tagliazucchi, L. Tassi, and G. Tosi, *Aust. J. Chem.*, **46**, 633 (1993).

3) F. Corradini, A. Marchetti, M. Tagliazucchi, L. Tassi, and G. Tosi, *J. Solution Chem.*, **23**, 777 (1994).

4) F. Corradini, A. Marchetti, M. Tagliazucchi, L. Tassi, and A. Varini, *Ann. Chim. (Rome)*, **85**, 267 (1995).

5) F. Corradini, A. Marchetti, M. Tagliazucchi, and L. Tassi, *Bull. Chem. Soc. Jpn.*, **68**, 3373 (1995).

6) T. Sigvartsen, B. Gestblom, E. Noreland, and J. Songstad, *Acta Chem. Scand.*, **43**, 103 (1989).

7) C. Tanford, in "The Hydrophobic Effect," J. Wiley, New York (1980).

8) M. Sakurai, K. Nakamura, and N. Takenaka, *Bull. Chem. Soc. Jpn.*, **67**, 352 (1994).

9) M. Sakurai, K. Nakamura, and K. Nitta, *Bull. Chem. Soc. Jpn.*, **67**, 1580 (1994).

10) A. Momchilov, V. Manev, A. Nasalevska, M. Pasquali, and G. Pistoia, *J. Appl. Electrochem.*, **20**, 763 (1990).

11) S. K. Ghosh and D. K. Hazra, *Indian J. Chem., Sect. A*, **29A**, 656 (1990).

12) E. Renard and J. C. Justice, *J. Solution Chem.*, **3**, 633 (1974).

13) M. V. Ramanamurti, P. V. S. S. Prabhu, and S. L. Bahadur, *Bull. Chem. Soc. Jpn.*, **59**, 2341 (1986).

14) "Paar Digital Density Meter-Instruction Manual," Graz, Austria (1984).

15) "Handbook of Chemistry and Physics," 66th ed, ed by R. C. Weast, CRC, Cleveland, OH (1985).

16) J. Gmehling, U. Ouken, and H. W. Schulte, *J. Chem. Eng. Data*, **25**, 29 (1980).

17) "Time Series Processor-TSP-User's Guide," ed by B. H. Hall, TSP International, Stanford, CA (1987).

18) C. F. Spencer and S. B. Adler, *J. Chem. Eng. Data*, **23**, 82 (1978).

19) J. P. E. Grollier, M. H. Karbalai Ghassemi, and A. Inglese, *Int. Data Ser. B*, Guideline **2C**, (1977).

20) O. Redlich and A. T. Kister, *Ind. Eng. Chem.*, **40**, 341 (1948).

21) V. Viti and P. Zampetti, *Chem. Phys.*, **2**, 233 (1973).

22) R. Lumry, E. Battistel, and C. Jolicoeur, *Faraday Symp. Chem. Soc.*, **17**, 93 (1982).

23) K. Aizawa and M. Kato, *J. Chem. Eng. Data*, **36**, 159 (1991).

24) J. L. Cabezas, S. Beltran, and J. Coca, *J. Chem. Eng. Data*, **36**, 184 (1991).